Postprint of: Jędrzejewska-Szczerska M., Wierzba P., Abou Chaaya A., Bechelany M., Miele P., Viter R., Mazikowski A., Karpienko K., Wróbel M., ALD thin ZnO layer as an active medium in a fiber-optic Fabry–Perot interferometer, Sensors and Actuators A: Physical, Vol. 221 (2015), pp. 88-94, DOI: 10.1016/j.sna.2014.11.001

ALD thin ZnO layer as an active medium in a fiber-optic Fabry-Perot interferometer

M. JĘDRZEJEWSKA-SZCZERSKA[1] , P. WIERZBA[1*], A. ABOU CHAAYA[2], M. BECHELANY[2], P. MIELE[2], R. VITER[3,4], A.MAZIKOWSKI[1], K. KARPIENKO[1], M.WRÓBEL[1]

[1]Gdańsk University of Technology, Department of Electronics, Telecommunication and Informatics, 11/12 Narutowicza, 80-233 Gdańsk, Poland

[2] Institut Européen des Membranes, UMR 5635 ENSCM UM2 CNRS, Université Montpellier 2, Place Eugène Bataillon, 34095 Montpellier, France

[3] Experimental physics department, Odessa National I.I. Mechnikov University, 42, Pastera str., 65026, Odessa, Ukraine

[4]Institute of Atomic Physics and Spectroscopy, University of Latvia, 19 Raina Blvd., LV 1586, Riga, Latvia

Abstract

A novel optical fiber sensor of temperature using a thin ZnO layer fabricated by Atomic Layer Deposition (ALD) is demonstrated for the first time. The thin ZnO layer was grown on the face of a standard optical telecommunication fiber SMF-28 and operates as a Fabry-Perot interferometer sensitive to temperature. The interferometer characterization was made in the temperature range extending from 50 to 300°C with resolution equal to 1°C. The output signal was analyzed by measurement of the shift of the maxima in spectral pattern. The sensitivity of temperature measurement is about 0.05 nm/°C. Furthermore, very good linearity of the sensor was achieved with correlation coefficient R^2 = 0.9984.

Keywords: Fiber-optic sensor; Atomic Layer Deposition; Zinc oxide; Fabry-Perot interferometer;

1. Introduction

Optical fiber sensors are successfully used not only in research laboratories but also in medicine and in many areas of industry. They can measure various physical quantities, especially: temperature, humidity and distance [1-4]. Fiber optic sensors possess unique advantages such as: immunity to electromagnetic field, small dimensions and light weight. At present, fabrication of an optical fiber sensor with the commonly used devices can be simple and inexpensive, which makes the use of fiber optic sensor more attractive than ever. Therefore, there is a need for materials that could serve as a

sensing layer in optical fiber sensors. Such layer must be sensitive to changes, in a selected physical quantity, and it must have a good adhesion to an optical fiber (usually to a silica glass fiber of diameter of 125 μm) [5,6].

On the other hand, in recent years, Zinc oxide (ZnO) has drawn attention of many researches as a very promising semiconducting material. Usually, the researchers focus on the use of electro-optical properties of ZnO, which can be used in optoelectronic devices, such as optoelectronic modulators [7,8]. The other, common use of ZnO layer is in the field of opto-chemical gas [9,10] or humidity sensors [11]. Application of ZnO layers in optical fiber sensors as a sensing medium, usually requires utilization of a physical phenomenon such as a Surface Plasmon Resonance [12] (which requires functionalization of sensor's surfaces) or the extensive use of specialized components such as dedicated planar waveguide [13] or expensive sapphire fiber [14].

Ultrathin ZnO films have been synthesized using different deposition techniques such as sol-gel, chemical vapor deposition, electrodeposition, RF sputtering and atomic layer deposition [15]. Among these techniques ALD appears to be one of the most promising techniques due to its simplicity, reproducibility and the high conformity of the obtained films. ALD is an innovative deposition technique which allows the fabrication of metal oxide thin films with tunable structural properties (thickness, grain size, chemical composition, texture, surface morphology and defect concentration). These properties are tailored by changing process conditions such as temperature, thickness or doping, as well as by selection of the substrate material [16,17], and have a strong impact on optical, mechanical, electrical and other fundamental properties of the ZnO layers [18,19].

In this paper, an optical fiber sensor based on ZnO thin film for temperature measurement is presented. The sensor employs low-coherence interferometry techniques to interrogate a Fabry-Perot sensing interferometer filled with ZnO thin film, deposited by the use of Atomic Layer Deposition (ALD) on the end-face of the standard single-mode optical fiber (SMF–28). In order to attain the best metrological parameters of the setup, the transmission function of the Fabry-Perot interferometer was analyzed and its construction was optimized.

2. Theory

The Zinc oxide thin films can be used in two basic extrinsic Fabry-Perot fiber interferometer types, as shown in Fig. 1. The cavity mirrors M1 and M2 use Fresnel reflection at the boundary between the ZnO layer and the surrounding medium (i.e. optical fiber or air).

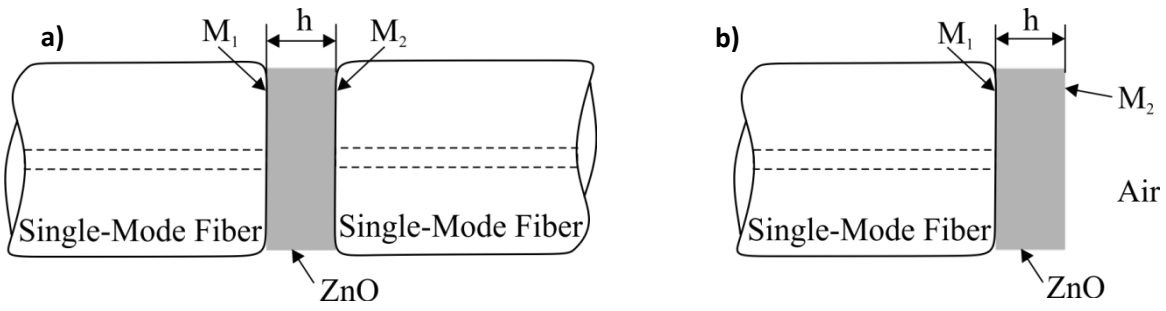

Fig. 1. Fabry-Perot interferometer with the cavity made of a ZnO layer: a) symmetric configuration, b) asymmetric configuration; *h* – thickness of the cavity, M_1, M_2 – cavity mirrors.

The Fabry-Perot interferometer in symmetric configuration, shown in Fig. 1a, can work both in the transmission and the reflection mode, while the asymmetric configuration, shown in Fig. 1b, can be used only in the reflection mode. The latter configuration is much more versatile, as it has a greater contact area with the surrounding medium and provides free access to the mirror M_2. What is also significant, the transmission function of a Fabry-Perot interferometer with optimized parameters can be approximated by a two-beam interferometer, which simplifies measured signal processing [20]. Therefore, for further analysis authors decided to use the Fabry-Perot interferometer in an asymmetric configuration.

For mathematical description, the following assumptions were made:

1^0 the deposited ZnO films do not exhibit the birefringence;

2^0 the refractive index of the ZnO films in the spectral region of interest, i.e. from about 600 nm to about 1600 nm, changes from 2.00 to 1.89, whilst the refractive index of media surrounding such film will be assumed to be lower than that of ZnO;

3^0 thickness of the film deposited on the fiber end-face is limited to 310 nm. Therefore, when such a film is illuminated by a near-Gaussian beam from a single mode fiber, the diameter of the beam does not increase appreciably in its path in the interferometer.

Based on the above assumptions, it is possible to describe the Fabry-Perot interferometer using traditional plane wave model, where the amplitudes of the Gaussian beams incident on and propagating in the interferometer are described by the formulas derived for plane waves. The analysis of the asymmetric Fabry-Perot interferometer, presented in Fig. 1b, is complicated, as the reflectivities of mirrors M_1 and M_2 are no longer equal. The reflectivity $\mathcal{R}_1$ of mirror M_1 is given by [21]:

$$\Re_1 = \left(\frac{n_2 - n_1}{n_2 + n_1} \right)^2 \tag{1}$$

where: n_2 – the refractive index of the ZnO layer and n_1 – effective refractive index of the fiber.

Similarly, reflectivity $\Re_2$ of mirror M is given by [21]:

$$\Re_2 = \left(\frac{n_2 - n_3}{n_2 + n_3} \right)^2 \tag{2}$$

where: n_3 – the refractive index of the surrounding medium (e.g. air).

Assuming that ZnO has higher refractive index than the two media surrounding it and employing the same technique as that presented in chapter 7.6 of [21] for the case where $\Re_1 \neq \Re_2$, one can express reflectivity R of an asymmetric Fabry-Perot interferometer by [21]:

$$R = \frac{\Re_1 + \Re_2 - 2\sqrt{\Re_1 \Re_2}\cos\delta}{1 + \Re_1 \Re_2 - 2\sqrt{\Re_1 \Re_2}\cos\delta}, \tag{3}$$

where: $\Re_1$, $\Re_2$ – the reflectivity of the cavity mirror M_1 and M_2, respectively, ϕ – the phase difference given by [21]:

$$\phi = \frac{4\pi}{\lambda_0} nh, \tag{4}$$

where: λ_0 – the wavelength in vacuum, h – the thickness of the ZnO layer, n – the refractive index of the layer.

The refractive index of ZnO layer is given by [22]:

$$n^2 = 2.81418 + \frac{0.87968\,\lambda^2}{\lambda^2 - 0.3042^2} - 0.0711\,\lambda^2, \tag{5}$$

where: λ – the wavelength expressed in μm.

Based on the numerical model outlined above, calculation worksheets were created in MathCAD v. 11 and reflection characteristics of the asymmetric Fabry-Perot interferometer was calculated. The calculations of reflectivity R as a function of wavelength λ were again conducted for 250 nm layer thickness values. The results are presented in Fig. 2.

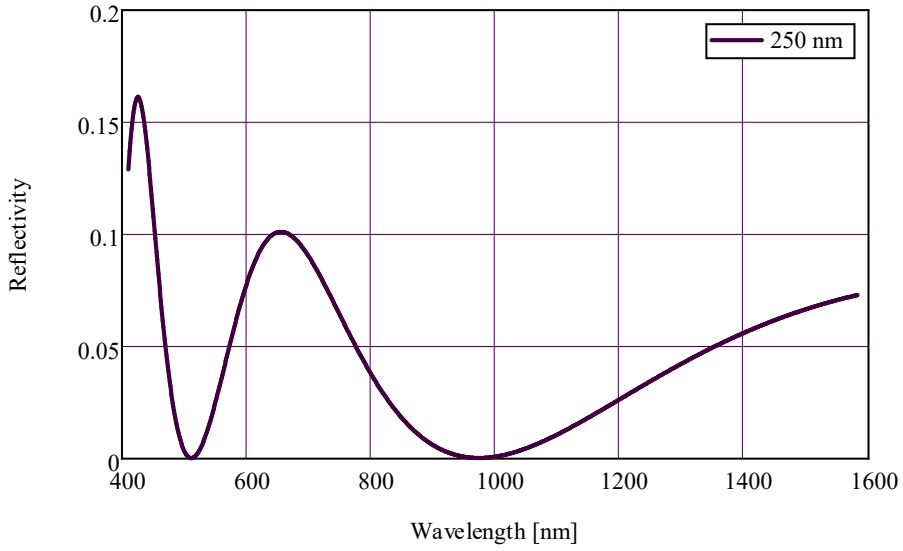

Fig. 2. Reflectivity R(λ) of an asymmetric Fabry-Perot interferometer with the cavity made by filled by a ZnO layer in the spectral range from 420 nm to 1580 nm.

The decrease of refractive index of the medium behind mirror M2, results in a substantial increase in reflectivity of the interferometer. It should be also noted that R(λ) does not fall to zero, because of substantial difference in reflectivity of mirrors M1 and M2.

Optical fiber Fabry-Perot sensing interferometers is seldom used as intensity sensors. Most commonly, the detection relies on spectral processing, implemented either using a broadband source and optical spectrum analyzer, or using a tunable laser and a detector, to minimize the impact of intensity fluctuations on the measurement result. More spectral processing techniques require at least half of the fringe to be covered by the spectrum of the source. In the case of considered ZnO films, such requirement can be fulfilled for the 250 nm film in the range of 650 nm – 1000 nm of wavelength.

3. Experimental

3.1. Preparation of ZnO thin layer by ALD

Diethyl Zinc (DEZ) ($Zn(CH_2CH_3)_2$, 95% purity, CAS: 557-20-0) was purchased from Sigma Aldrich. Silicon wafer p-type (100) was obtained from INSTITUTE OF ELECTRONIC MATERIALS TECHNOLOGY (Warsaw, Poland) and Glass substrates from ChemLand (Stargard Szczeciński, Poland), as well as SMF-28 optical fiber. Substrates were pre-cleaned in acetone, ethanol and de-ionized water for 5 min to remove organic contaminants. A custom-made ALD reactor was used for the synthesis of Zinc

oxide thin films. ALD was achieved using sequential exposures of DEZ and H_2O separated by a purge of nitrogen with a flow rate of 100 sccm. The deposition regime for ZnO consisted of 0.1 s pulse of DEZ, 20 s of exposure to DEZ, 40 s of purge with nitrogen followed by 2 s pulse of H_2O, 30 s of exposure to H_2O and finally 60 s purge with nitrogen. 1250 cycles were deposited on Si substrates, on glass substrates and optical fibers at 100°C.

3.2. Characterization of the sensing layer

Structural properties of ZnO films were characterized by Scanning electron microscopy (SEM), Ellipsometry, Energy-dispersive X-ray spectroscopy (EDX) and Grazing Incidence X-ray Diffraction (GIXRD). The morphology of the surface was studied using an Asylum Research MFP-3D Atomic Force Microscope, operating in tapping mode and equipped with a commercial silicon tip. The size of the AFM images was 3mm x 3mm. SEM measurements were performed using a Hitachi S-4800 microscope and EDX on Hitachi S-4500 coupled with a Thermofisher EDX detector. The thicknesses of ZnO layers were measured using a Semilab GES5E spectroscopic ellipsometer (extended visible: 1.23eV - 5eV). Structural characterizations by GIXRD were performed using Bruker D5000.

Optical properties on ZnO thin films have been studied with UV-VIS transmittance (UV-VIS spectrophotometer Shimadzu UV-1700, the spectral range 300-1100 nm, 1 nm step) and photoluminescence spectroscopy (the spectral range 370-800 nm). The excitation of luminescence was performed by a solid state laser source (Nd:YAG, LCS-DTL-374QT, Russia, 355 nm, 13 mW/cm^2). The registration of the emitted spectra was provided by an experimental setup described by Abou Chaaya *et al.* [23].

3.3. Measurement of metrological properties of the fiber optic ZnO sensor

In order to verify the possibility of using ZnO thin layer on the top of optical fiber as a Fabry-Perot temperature sensor, a series of test structures were manufactured [15] and tested. The structures consisted of a layer of ZnO grown using ALD on the end face of SMF-28 fiber. The designed thickness of the layer was 250 nm. The measurement system, used employed to test these structures, is shown in Fig. 3. It consists of a superluminescent diode (Superlum Broadlighter S930, Gaussian spectral density, λ_{MAX} = 932.4 nm, $\Delta\lambda_{FWHM}$ = 66.1 nm) acting as a light source, connected to the test structure by a single-mode fiber, an Ando AQ6319 optical spectrum analyzer with resolution bandwidth set to 1 nm working as the detection setup and temperature calibrator Ametek ETC-400A.

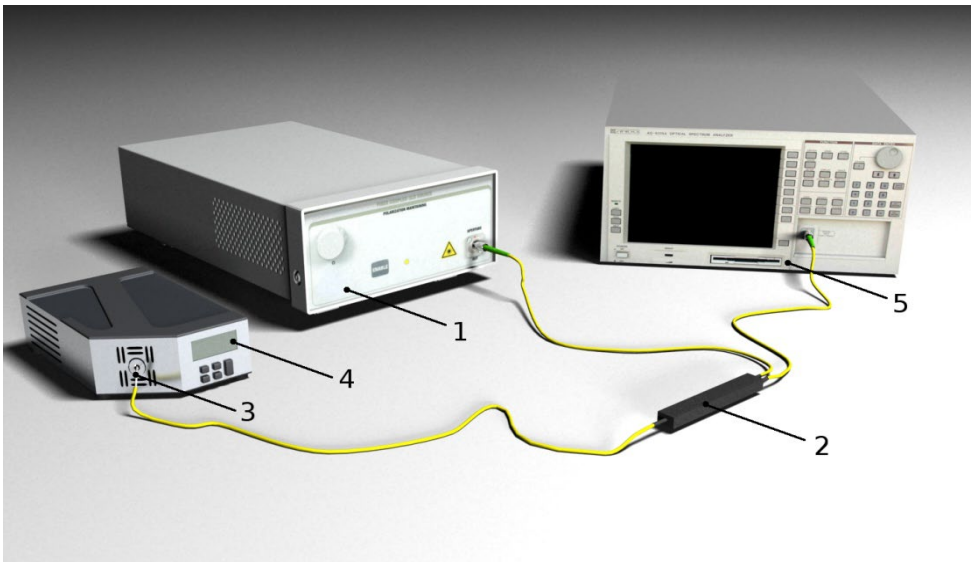

Fig. 3. The experimental set-up: 1) superluminescent diode; 2) fiber-optic coupler; 3) Fabry-Perot interferometer; 4) temperature calibrator; 5) optical spectrum analyzer.

In the elaborated test structures, phase difference between interfering beams reflected from the ZnO thin film surfaces depending on the temperature. Any change of the phase difference between interfering beams modifies the spectrum of reflected signal *I(v)* according to [23]:

$$I(\nu) = S(\nu)R(\nu) \tag{6}$$

where: *S(v)* – the spectral distribution of the light source; *R(v)* – reflectivity of the Fabry-Perot sensing interferometer.

4. Results and discussion

4.1. ZnO layer characterization

Fig. 4a shows the SEM images of ALD ZnO thin films deposited on Si substrates with 1250 cycles. The images indicate a conformal coating of the Si substrate by the ALD ZnO films. The ZnO films develop a rough surface with colonar growth. GIXRD diffraction patterns of ZnO thin films are shown in Fig. 4b. The SEM image confirms the 310 nm ZnO thickness calculated based on the growth per cycles for ZnO films observed elsewhere (GPA = 0.25 nm). GIXRD diffraction (Fig. 4b) shows peaks at 2θ = 31.74°, 34.42° and 36.22° respectively corresponding to (100), (002) and (101) of ZnO as generally observed with the ZnO thin films deposited by Abou Chaaya *et al.* [23]. The AFM image of ZnO film is shown in Fig. 4c. The sample showed good polycrystalline structure with well-shaped nanograins. The average size of the nanograins was 40-60 nm. The surface roughness value (Rms) was 2.82 nm. Transmittance spectra of ZnO layer is shown in Fig. 4d. The samples were transparent in the range of wavelengths 440-1100 nm. The absorption edge of the ZnO film at 340-440 nm is

typical for ZnO nanostructures. Optical density (OD=ln(1/T), where T is transmittance) was used for calculations of band gap [23, 25]. The band gap of ZnO film estimated according to Abou Chaaya *et al.* [23, 25] was 3.28 eV (Fig. 4e).

Room temperature photoluminescence spectrum of ZnO is shown in Fig. 4f. Two emission bands in UV and Visible range are observed. The analysis of the spectrum performed by Origin software showed single peak positions. The peaks in UV region at 3.3 eV, 3.25 eV and 3.16 eV correspond to free (FX), bound (D^0X) excitons and the phonon replica, respectively [24-26]. The peaks at Visible range at 2.24 and 1.9 eV correspond to the structural defects: oxygen vacancy and interstitial oxygen, respectively [15, 24].

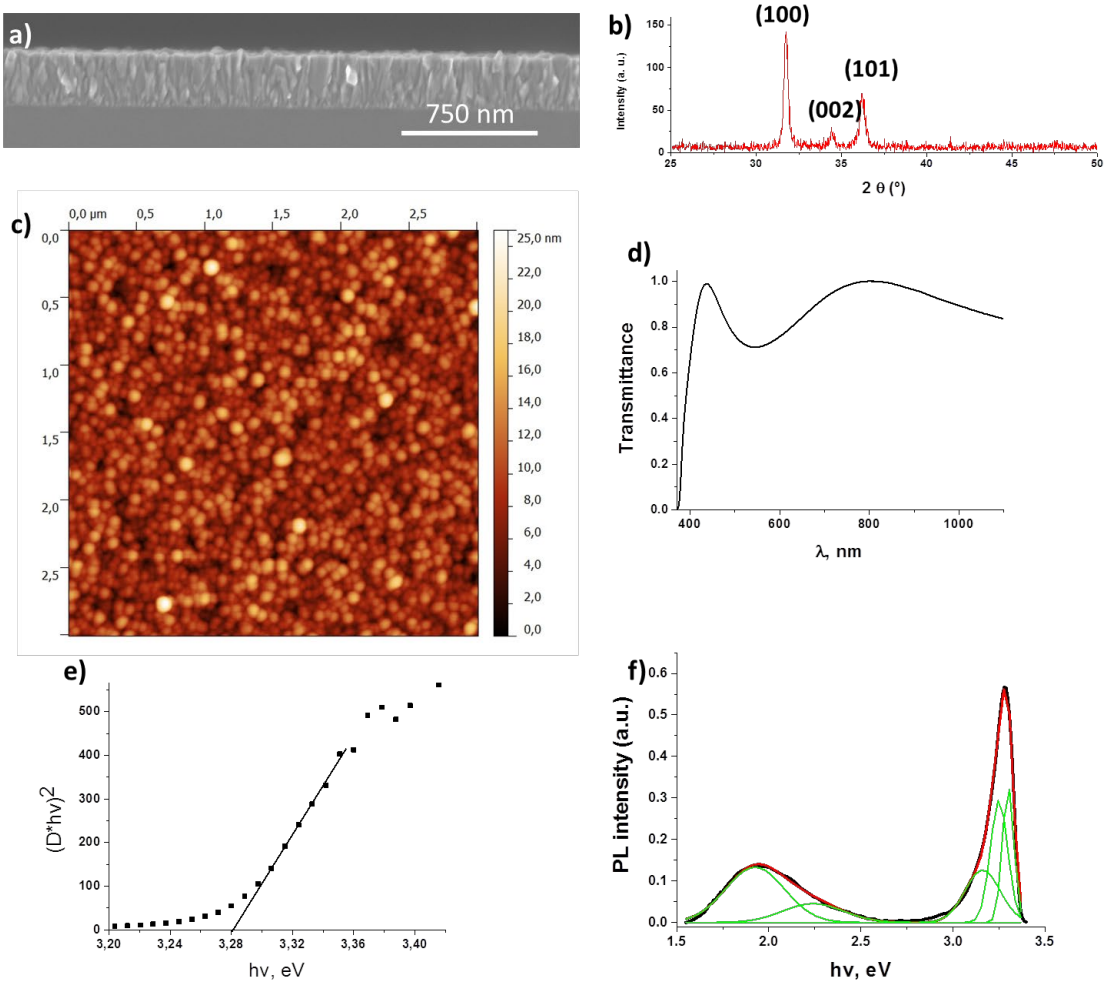

Fig. 4. The SEM cross section image of ZnO ALD films deposited on Si substrates with 1250 cycles, b) GIXRD, c) AFM image, d) Transmittance spectra, e) Band gap calculation of ZnO film and f) Room temperature photoluminescence spectrum of ZnO film.

4.2. Measured signal vs. temperature

The dependence of the measured signal spectra of presented interferometer on the temperature ranging from 50 to 300˚C is plotted in Fig. 5a and Fig. 5b. The positions of the maxima in the spectral pattern shift to shorter wavelengths during heating.

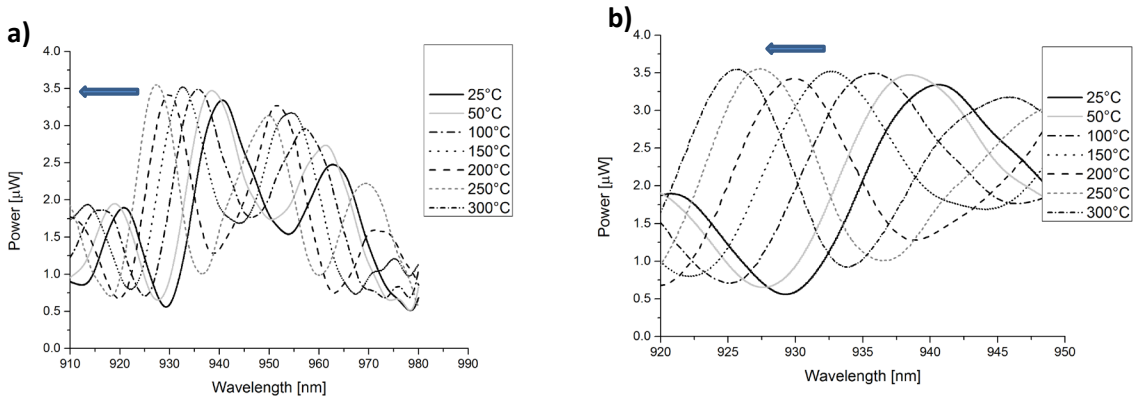

Fig. 5. The spectra of measured signal during heating: a) in full measured range (910 – 980 nm); b) in the range of 920 to 950 nm.

Similarly, the spectra of the measured signal acquired during cooling (from 300 to 50 ˚C) are shown in Fig. 6.

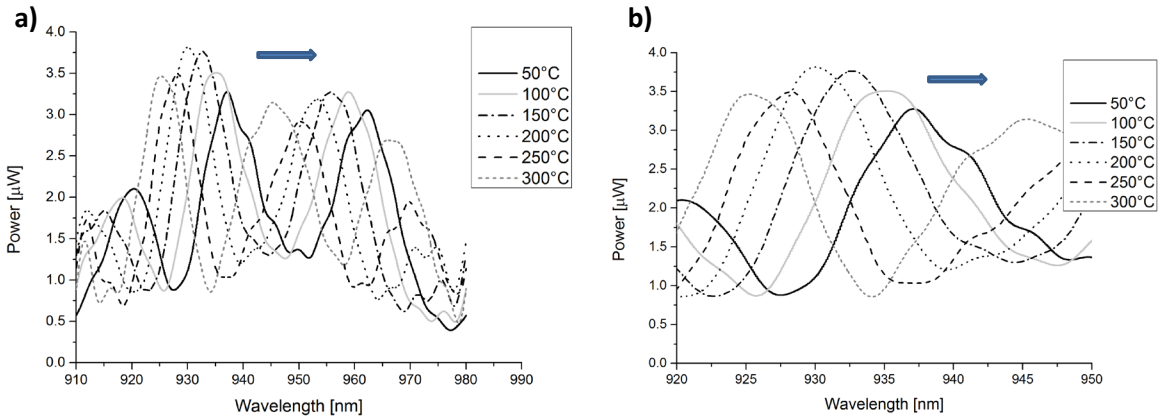

Fig. 6. The spectra of measured signal during cooling: a) in full measured range (910 – 980 nm); b) in the range of 920 to 950 nm.

It can be noted that the position of maxima in the spectral pattern shift to the longer wavelengths during cooling.

The dependence of the position of maxima in the spectral pattern on the temperature during cooling and heating is shown in Fig.6. It should be noticed that the maximum position changing per temperature unit is almost constant over the investigated range.

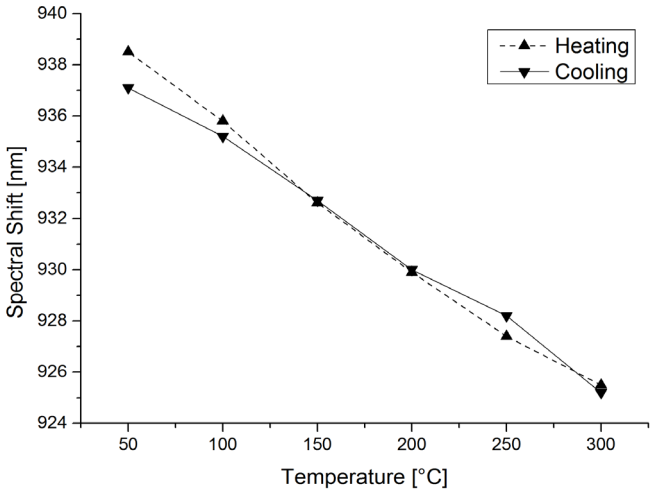

Fig.7. The dependence of the spectral shift of measured signal on the temperature.

The interferometer characterization was made in the temperature range extending from 50 to 300°C with resolution equal to 1°C. The output signal was analyzed by measurement of the shift of the maxima in spectral pattern. The shift of the investigated maxima of the spectral pattern equal to 13 nm was achieved in investigated temperature range, thus the obtained sensitivity of temperature measurement can be estimated as about 0.05 nm/°C. Furthermore, we achieved very good linearity of the sensor with correlation coefficient $R^2 = 0.9984$.

The main difficulty during experiment was associated with analysis of the measurement signal, as the SMF-28 fiber working at the wavelength of λ = 932.4 nm caused it to support the propagation of two modes. This resulted in the interference of the two modes on the detector, seen in Fig. 4 and Fig. 5, as periodic fringes modulating the reflectance spectrum. This modulation does not impair the measurement process.

Taking into account the above results, we can say that the investigation of the ALD ZnO layer as an active medium in the fiber-optic Fabry-Perot interferometer confirms its viability of the temperature measurement with acceptable metrological parameters.

5. Conclusions

In this article the use of ALD ZnO thin layer as an active medium of Fabry-Perot interferometer has been presented. The dependence of the fiber-optic interferometer signal on temperature changes in the low-coherence measurement set-up with signal processing in spectral domain was investigated. The asymmetric configuration of the Fabry-Perot interferometer working in reflective mode was implemented. This interferometer was chosen because of its advantages: relatively simple configuration, potentially low cost, high resolution. Furthermore, because of its small size, it is possible to make nearly point-wise temperature measurement.

The investigation of the ALD ZnO layer as an active medium in the fiber-optic Fabry-Perot interferometer confirms its ability to measure temperature with acceptable/good measurement parameters. For the first time, the fiber-optic temperature interferometric sensor in Fabry-Perot configuration was built with a ALD ZnO 250 nm-thick layer on the top of a conventional SMF-28 fiber. Presented preliminary results form the basis for building a temperature sensor ready for practical applications.

Acknowledgements

This study was partially supported by the FNP project under grant no. 173/UD/SKILLS/2012, National Science Center, Poland grant no. 2011/03/D/ST7/03540 and DS Projects of the Faculty of Electronics, Telecommunications and Informatics, Gdańsk University of Technology, as well as FOTONIKA - LV (FP7- REGPOT -CT-2011-285912) BIOSENSORS-AGRICULT (PIRSES-GA-2012-318520).0

References

1. K.T.V. Grattan, B.T. Meggitt, Optical Fiber Sensor Technology, Kluwer Academic Publisher, Boston, 2000.
2. J. Lopez-Higurea, Handbook of Optical Fiber Sensing Technology, Wiley, New York, 2002.
3. P. Venancio, R. Cottis, R. Narayanaswamy *et al.*, Optical sensors for corrosion detection in airframes, Sensors Actuat. B-Chem. 182 (2013) 774-781.
4. K.Bohnert, P. Gabus, J. Kostovic, *et al.*, Optical fiber sensors for the electric power industry, Opt. Laser Eng. 43 (2005) 511-526.
   DOI: 10.1016/j.optlaseng.2004.02.008
5. R. Bogdanowicz, M. Smietana, M. Gnyba *et al.*, Nucleation and growth of CVD diamond on fused silica optical fibres with titanium dioxide interlayer, Phys. Status Solidi A 210 (2013) 1991-1997.
   DOI: 10.1002/pssa.201300096
6. M. Jędrzejewska-Szczerska, R. Bogdanowicz, M. Gnyba *et al.*, Fiber-optic temperature sensor using low-coherence interferometry, Eur Phys J –ST 154 (2008) 107-111.
7. G. Fox, N. Setter, H. Limberger, Fabrication and structural analysis of ZnO coated fiber optic phase modulators, J. Mater. Res. 11 (1996) 2051-2061.
8. R. Heideman, G. Veldhuis, E. Jager *et al.*, Fabrication and packaging of integrated chemo-optical sensors, Sensors and Actuat. B: Chem. 35-36 (1996) 234-240.

9. P. Struk, T. Pustelny, K. Gołaszewski *et al.,* Gas Sensors Based on ZnO structures, Acta Phys. Pol. A 124 (2013) 567-569.
10. B. Renganathan, D. Sastikumar, G. Gobi G. *et al.*, Nanocrystalline ZnO coated fiber optic sensors for ammonia gas detection, Opt. Laser Technol. 43 (2011) 1398-1404. DOI:10.1016/j.optlastec.2011.04.008
11. S. Shukla, T. Sshutosh, G. Parashar *et al.*, Exploring fiber optic approach to sense humid environment over nano-crystalline zinc oxide film, Talanta 80 (2009) 565-571. DOI: 10.1016/j.talanta.2009.07.026
12. A. Sharma, B. Gupta, Metal-semiconductor nanocomposite layer based optical fiber surface plasmon resonance sensor, J. Opt. A: Pure Appl. Opt. 9 (2007) 180-185. DOI: 10.1088/1464-4258/9/2/011
13. P. Struk, T. Pustelny, K. Gut *et al*., Planar Optical Waveguides Based on Thin ZnO layers, Acta Phys. Pol. A 116 (2013) 414-418.
14. P. Cai, D. Zhen, X. Xu *et al.*, A novel fiber-optic temperature sensors based on high temperature-dependent optical properties of ZnO film on sapphire fiber-ending, Mater. Sci. Eng. B 171 (2010) 116-119. DOI: 10.1016/j.mseb.2010.03.083
15. A. Abou Chaaya, R. Viter, M. Bechelany *et al.*, Evolution of microstructure and related optical properties of ZnO grown by atomic layer deposition, Beilstein J. Nanotech. 4 (2013) 690-698.
16. J .Elias, M. Bechelany, I. Utke *et al.,* Urchin-inspired zinc oxide as building blocks for nanostructured solar cells, Nano Energy 1 (2012) 696-705.
17. J. Elias, I. Utke, S. Yoon *et al.,* Electrochemical growth of ZnO nanowires on atomic layer deposition coated polystyrene sphere templates, Electrochim. Acta 110 (2013) 387-392.
18. R. Raghavan, M. Bechelany, M. Parlinska *et al.,* Nanocrystalline-to-amorphous transition in nanolaminates grown by low temperature atomic layer deposition and related mechanical properties, Appl. Phys. Lett. 100 (2012) 19.
19. A. Abou Chaaya, R. Viter, I. Baleviciute *et al.,* Tuning Optical Properties of Al2O3/ZnO Nanolaminates Synthesized by Atomic Layer Deposition, J. Phys. Chem. C 118 (2014) 3811-3819.
20. P. Wierzba, M. Jędrzejewska-Szczerska, Optimization of a Fabry-Perot Sensing Interferometer Design for an Optical Fiber Sensor of Hematocrit Level, Acta Phys. Pol. A 124 (2013) 586-588.
21. M. Born , E. Wolf, Principles of Optics, 6th Ed. Pergamon Press, Oxford, 1994.
22. http://refractiveindex.info/?group=CRYSTALS&material=ZnO
23. P. Hariharan, Optical Interferometry, 2nd Edition, Academic Press Elsevier Science, San Diego 2003.
24. A. Chaaya, R. Viter, I. Baleviciute *et al.*, Tuning Optical Properties of Al_2O_3ZnO Nanolaminates Synthesized by Atomic Layer Deposition, J. Phys. Chem. C 118 (2014) 3811–3819.
25. R. Viter, V. Khranovskyy, N. Starodub *et al.,* Application of Room Temperature Photoluminescence From ZnO Nano-rods for Salmonella Detection, IEEE Sen. J. 14 (2014) 2028-2034.
26. V. Khranovskyy, G. R. Yazdi, G. Lashkarev *et al.*, Investigation of ZnO as a perspective material for photonics, Phys. Status Solidi A, 205 (2008) 144–149.